

Journal of Biomedical Optics

SPIEDigitalLibrary.org/jbo

Crude extract of *Fusarium oxysporum* induces apoptosis and structural alterations in the skin of healthy rats

Luis F. de Paulo
Ana C. Coelho
Terezinha I. E. Svidzinski
Francielle Sato
Jurandir H. Rohling
Maria Raquel M. Natali
Mauro L. Baesso
Luzmarina Hernandez

Crude extract of *Fusarium oxysporum* induces apoptosis and structural alterations in the skin of healthy rats

Luis F. de Paulo,^a Ana C. Coelho,^a Terezinha I. E. Svidzinski,^b Francielle Sato,^c Jurandir H. Rohling,^c Maria Raquel M. Natali,^a Mauro L. Baesso,^c and Luzmarina Hernandez^a

^aUniversidade Estadual de Maringá, Departamento de Ciências Morfológicas, Avenue Colombo 5790, Maringá, Paraná, Brazil

^bUniversidade Estadual de Maringá, Departamento de Ciências Básicas da Saúde, Avenue Colombo 5790, Maringá, Paraná, Brazil

^cUniversidade Estadual de Maringá, Departamento de Física, Avenue Colombo 5790, Maringá, Paraná, Brazil

Abstract. We evaluate the biological and physicochemical effects of a *Fusarium oxysporum* crude extract (CE) on the skin of healthy rats. The CE is topically applied and subsequently the skin is collected after 3, 6, 12, and 24 h. The samples are analyzed by Fourier transform infrared photoacoustic spectroscopy (FTIR-PAS) and histomorphometric analysis. Terminal dUTP nick end labeling (TUNEL assay) is performed to detect both the cells in apoptosis and proliferation. There is a thickening of the epidermis after 6, 12, and 24 h and dermis after 12 and 24 h of CE application. A reduction of the dermis thickness is observed at 3 and 6 h. The treated skin shows higher labeling intensity by TUNEL at 3 h, while a higher intensity by proliferating cell nuclear antigen occurs at 3 and 12 h. FTIR-PAS data support the histology observations showing an increase in the absorption peaks in the dermis after the application of the CE. *F. oxysporum* CE permeated through the epidermis and the dermis, reaching the subcutaneous tissue, inducing cell apoptosis, and causing physicochemical changes in the organic molecules located in the dermis. This is the first known study associating histopathological and physical chemistry changes on healthy skin after the application of *F. oxysporum* CE. © 2013 Society of Photo-Optical Instrumentation Engineers (SPIE) [DOI: 10.1117/1.JBO.18.9.095004]

Keywords: *Fusarium oxysporum*; mycotoxin; skin infection; Fourier transform infrared photoacoustic spectroscopy.

Paper 130456RR received Jul. 3, 2013; revised manuscript received Aug. 21, 2013; accepted for publication Aug. 22, 2013; published online Sep. 26, 2013.

1 Introduction

The genus *Fusarium* is a well-known plant pathogen that causes damage to agriculture.^{1,2} Over the past 30 years, the *Fusarium* species have been intensively studied and of the 61 identified species, at least 35 are known to produce mycotoxins that are harmful to animals and humans.^{3–8}

The *Fusarium* mycotoxins are known as chemically different secondary metabolites. These mycotoxins can contaminate cereal grains causing disease and death in the animals that consume them. The trichothecenes [T2 toxin, deoxynivalenol, nivalenol, fusarenon-X (FX), and diacetoxyscirpenol (DAS)], fumonisins, zearalenone, and moniliformin are the most important *Fusarium* mycotoxins.^{9,10} These mycotoxins cause neurological damage and are frequently associated with animal and human diseases.^{4,5} Several mycotoxins are stable under normal food-processing conditions; thus, they may be present in natural foods and processed products.^{11,12}

Individuals who consume contaminated food are not exposed to a single mycotoxin; rather, they are exposed to a cocktail of them.¹³ *In vitro* experiments have shown that a mixture of mycotoxins results in additive toxicity or synergy that reduces the effective toxic dose of each component in the mixture.^{14,15} If this potentiating occurs *in vivo*, then the health consequences will be more severe.

In humans, the species *Fusarium* may cause local, invasive, or disseminated infections. The pathogen typically affects immunocompromised individuals because infections in

immunocompetent individuals are reported less frequently.^{16,17} Among immunocompromised patients, *Fusarium* is the second most common cause of fungal infection, with an increased incidence in patients with hematologic malignancies and especially in those exposed to recipients of hematopoietic stem cell transplantations.¹⁸

The entry points to the disseminated infection include the respiratory tract, gastrointestinal tract, and skin.¹⁶ Skin lesions, which are typically located on the extremities, are often described as painful subcutaneous nodules that may ulcerate and become necrotic lesions of the gangrenous erythema type.¹⁸ For skin infections, the entry points are wounds, digital ulcers, onychomycosis, and paronychia.^{17,19–21}

In recent years, the number of *Fusarium* onychomycosis cases in immunocompetent patients has increased significantly.^{17,22} Guilhermetti et al.¹⁷ reported a 7.5% incidence of confirmed cases of onychomycosis by *Fusarium* spp. and *Fusarium oxysporum* (*F. oxysporum*). The latter is one of the most common and pathogenic of the genus *Fusarium* and is the specie that has been mostly isolated.^{18,22}

In humans, this specie is an important emerging pathogen due to the increasing number of severe cases reported and its wide-ranging resistance to antifungal drugs.^{23,24} The increase in *F. oxysporum* infections in immunocompetent patients is an important aspect; thus, the evaluation of the biological and physicochemical effects of *F. oxysporum* on the skin of healthy rats and their relation with induced apoptosis is of utmost importance.

Address all correspondence to: Francielle Sato, State University of Maringá, Department of Physics, Avenue Colombo 5790, 87020-900, Maringá, Paraná, Brazil. Tel: +55-44-30115917; Fax: +55-44-32634623; E-mail: fsato@uem.br

It is well recognized that techniques based on infrared radiation provide an important route to access chemical bonding information of biological tissues.^{25–30} This can be done by exploring the finger print characteristics of the optical absorption bands in this spectral region. Among these methods, Fourier transform infrared photoacoustic spectroscopy (FTIR-PAS) has the special characteristic of allowing depth profile studies to detect the penetration and interaction of substances in biological tissues.^{31–33} It can be applied for measurements at clinical conditions because minimal sample preparation is needed. It is a nondestructive method and permits inspection in opaque and highly scattering samples.

Therefore, the aim of this study was to investigate the biological and physicochemical effects of a crude extract (CE) of *F. oxysporum* on the skin of healthy rats. The FTIR-PAS spectroscopy was applied to evaluate the induced physicochemical structural changes and their relation with the occurrence of apoptosis.

2 Materials and Methods

The study protocol was reviewed and approved by the Local Ethics Committee for Animal Experimentation of the Universidade Estadual de Maringá (UEM), under protocol number 005/2010 and statement 080/2010.

2.1 Fungal Isolate and Culture Conditions

The *F. oxysporum* sample used in this study was previously isolated from an onychomycosis patient at the Teaching and Research Laboratory of the Departamento de Ciências Básicas da Saúde, UEM, Maringá, Paraná, Brazil. The fungus was peaked in Petri dishes containing potato dextrose agar and incubated for 7 days at 25°C. Three 5-mm discs were removed from the culture and placed into flasks containing 200 mL of Czapek–Dox (CZ) medium, which had been adjusted to a pH of 5.5 and sterilized at 120°C for 20 min. The flasks were maintained at a 70-rpm orbital agitation during 15 days at 25°C.

Next, the culture was sterilized at 120°C for 20 min and filtered with Whatman filter paper No. 1 for mycelium removal. The filtration product was sterilized on a Millipore filter with a 0.45- μm pore size and dialyzed against the distilled water overnight. The obtained extract, referred to as CE, was maintained at 4°C until use. As an experimental control, 100 mL of CZ medium were produced and exposed to the same condition as that used for the fungus-containing medium.

2.2 Experimental Procedures

Male Wistar rats weighing 150 to 200 g were used. The animals were kept in polypropylene boxes at a ratio of four animals/box in an environment with a controlled temperature of $22 \pm 2^\circ\text{C}$, 50% humidity, and a light-dark cycle of 12 h, with water and food *ad libitum*.

While under anesthesia with sodium thiopental (40 mg/kg), an area of 1.5 cm² on the back, near the cervical region of each animal, was epilated 2 days before the topical application of the solutions. This procedure was adopted in order to avoid inflammatory reaction that would interfere in the results interpretation. On the day of the experiment, 50 μL of the CE or 50 μL of the CZ medium were topically applied to each animal of the experimental and control groups, respectively. The animals were sacrificed 3, 6, 12, and 24 h after the application of the solutions.

2.3 Physicochemical Analysis of the Skin by FTIR-PAS

For the physicochemical analysis of the skin following topical application of either the CE or the CZ medium, two animals/time were used for each experimental group. After each animal sacrifice, the skin containing both epidermis and dermis was removed and sent immediately for *ex vivo* analysis using an FTIR spectrometer (Varian, Model 7000) equipped with an MTEC model 300 photoacoustic detection cell. Each skin sample was positioned inside the cell chamber with its epidermal side upside down allowing the radiation to excite the dermal region, the opposite side in relation to where the CE or the CZ medium was applied, as illustrated in Fig. 1. After that the cell chamber was purged with the helium gas for approximately 5 min to remove air moisture, and subsequently it was sealed to perform the measurements. This procedure increases the sensitivity of the technique and minimizes spectral interference from loosely bonded molecules of the air such as CO₂. All the spectra were collected in the rapid scan mode in the spectral range between 4000 and 400 cm⁻¹, with 4 cm⁻¹ resolution, an average of 28 scans and the interferometer mirror velocity (v) of 0.64 cm/s (10 kHz). The reference spectrum was acquired by the use of a carbon black sample.

The depth analysis in the sample was estimated through the thermal diffusion length (cm) as $\mu = [D\lambda/(2\pi v)]^{1/2}$, in which D is the sample thermal diffusivity (cm²/s) and λ is the incident radiation wavelength (cm). This parameter is the dimension over which the thermal wave decays to 1/ e of its original amplitude and can be used in the analysis as approximately the sampling depth where the PAS signal is generated. In our experimental

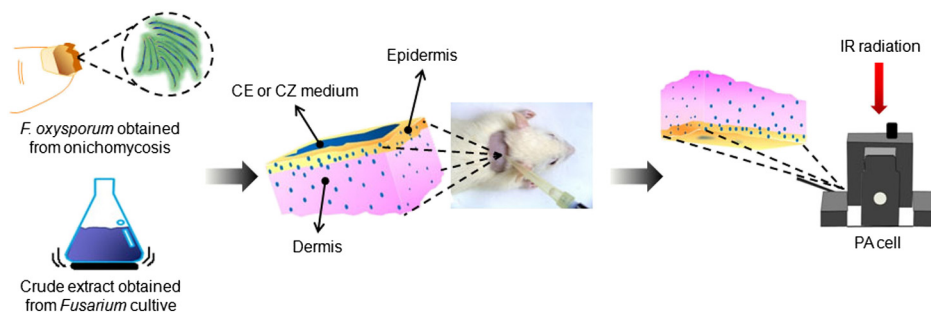


Fig. 1 Representation of the skin topical application of the *Fusarium oxysporum* crude extract (CE) or Czapek–Dox (CZ) culture medium, and the sample positioning in the photoacoustic cell.

conditions, using the skin thermal diffusivity measured before as $4.1 \times 10^{-4} \text{ cm}^2/\text{s}$ (Ref. 34) and $v = 0.64 \text{ cm/s}$, we can calculate the values of μ according to the incident radiation wavelength, being, e.g., $2.8 \text{ }\mu\text{m}$ at 1250 cm^{-1} and $1.7 \text{ }\mu\text{m}$ at 3850 cm^{-1} . Therefore, since the exciting radiation was incident on the dermal side of the skin and the application of the CE and CZ medium was done on the epidermal side, the detection of optical bands would be an indication that the formulation penetrated throughout the skin.

2.4 Histological Study

The histological studies were performed in four animals for each time interval after the formulations' application in both experimental and control groups. After killing, the skin was collected and fixed in 4% paraformaldehyde for a period of 24 h. The skin was then processed for paraffin embedding. Semi-serial $7\text{-}\mu\text{m}$ thick sections were prepared and placed on slides. The samples were used for the following techniques: (a) hematoxylin and eosin (H&E) staining for the morphological observation and morphometric analysis of the epidermis and dermis thickness; (b) sirius red (picro sirius) staining for the analysis of the area occupied by collagen in the dermis; (c) immunohistochemical *in situ* detection of fragmented DNA [terminal dUTP nick end labeling (TUNEL assay)] for the analysis of apoptosis in the epidermis and dermis; and (d) immunohistochemistry using anti-proliferating cell nuclear antigen (PCNA) to study the cell proliferation in the epidermis and dermis.

2.4.1 Histomorphometric measurements

The skin morphology was observed microscopically to study the occurrence of histopathological alterations, such as the presence of inflammatory infiltrations or epidermis or dermis structure alterations. The inflammatory reaction was graded as absent (–), weak (+), moderate (+ +), or severe (+ + +) in accordance with the frequency of cells in the dermis. Ten histological sections/animals were analyzed. The observations were performed with an Olympus BX41 microscope adopting the double-blind method. The two different researchers who made the observations did not know which slides contained the control or the treated skins.

For the morphometric analysis of the epidermis and dermis thicknesses, histological section images were captured using an Olympus BX41 optical microscope with a $10\times$ objective coupled to a QColor 3 Olympus camera. The measurements were acquired using the Image Pro Plus® software, version 4.5 (Media Cybernetics). The images from 10 sections/animals were analyzed, and 200 measurements/animals were separately recorded for the epidermis and dermis. The results are expressed as the mean \pm standard error.

2.4.2 Analysis of area covered by the collagen fibers of the dermis

The analysis of the collagen fibers of the dermis was performed by light microscopy using optical polarization. This method based on birefringence allows the collagen to be classified as type I or III. For the morphometric analysis of the area covered by collagen, standardized images of 12 fields of 0.8 mm^2 /animals were captured with a $20\times$ objective. The image capture was performed with the same illumination intensity and was digitized and analyzed with the Image Pro Plus® software

(Version 4.5, Media Cybernetics). The results are expressed as the mean \pm standard error in μm^2 .

2.4.3 *In situ* detection of fragmented DNA—terminal dUTP nick end-labeling (TUNEL assay)

DNA fragmentation was examined using an apoptosis detection kit (ApopTag® Peroxidase, Chemicon). After deparaffinization and rehydration, the slides containing the histological sections were subjected to enzymatic digestion with $20 \text{ }\mu\text{g/mL}$ of proteinase K for 5 min, treated with 5% hydrogen peroxide (30 volumes) for 20 min to block endogenous peroxidase, and washed with 0.1 M PBS with pH 7.4. The sections were then immersed in equilibration buffer for 10 min and incubated with a solution containing the enzyme terminal deoxynucleotidyl transferase at 37°C for 1 h. The sections were washed in PBS and incubated with the conjugated anti-digoxigenin peroxidase and peroxidase substrate to detect apoptosis signs stained in brown. Counterstaining was performed with Harris hematoxylin. The immunostaining on the epidermis and dermis was performed based on the frequency of the cells stained adopting the following classification: absent (–), weak (+), moderate (+ +), or strong (+ + +).

2.4.4 Identification of cells under proliferation (PCNA)

The detection of cells undergoing proliferation was performed using the primary antibody anti-PCNA (Zymed). After deparaffinization and rehydration, the histological sections were subjected to antigenic recovery in a citrate buffer with a pH of 6.0. The primary antibody anti-PCNA (1:100) was incubated for 60 min at room temperature (RT). A commercial kit (Histostain® Plus Mouse Primary DAB Zymed) was used at RT for detection. The sections were counterstained with Harris hematoxylin. The immunostaining on the epidermis and dermis was classified as absent (–), weak (+), moderate (+ +), or strong (+ + +) based on the frequency of the cells stained.

2.4.5 Statistical analysis

The results of the collagen-covered area and skin thicknesses were subjected to statistical treatment. All the data were analyzed with Kolmogorov–Smirnov, D'Agostino and Pearson, and Shapiro–Wilk normality tests. When the data did not have a normal distribution, an analysis of variance and the Kruskal–Wallis nonparametric test along with the Dunn post test were used. A 5% significance level was used ($P < 0.05$).

3 Results and Discussion

The obtained CE is a complex mixture produced by fungus growth, which includes metabolism products such as secondary metabolites like mycotoxins. The extract also contains partially digested culture medium residue components. The spectral analyses of organic compounds by FTIR represent a method for obtaining a “fingerprint” of the molecules, i.e., allowing for their identification from the recognition of the functional groups to which they belong. The bands between 1700 and 1500 cm^{-1} have been related to amides I and II, and they are frequently used as an indicator of secondary protein structure.^{35,36} The bands between 3000 and 2830 cm^{-1} are related to the symmetric and asymmetric stretching of —C—H groups in proteins and lipids^{36,37} and those between 3800 and 3000 cm^{-1} to the OH^- and amine (N—H) molecules.³⁶ It is known that the identification of

amides I and II and —C—H groups may allow the monitoring of conformational changes detected by the vibrational variations of these molecules when subjected to a state different from that considered in physiological tests.³⁸

Figures 2(a) and 2(b) show the FTIR-PAS absorption spectra between 1900 and 1250 cm^{-1} of the dermis of rats without the application of any substance and at 3, 6, 12, and 24 h after the topical application of both CZ culture medium or *F. oxysporum* CE. The changes in the absorption bands suggest structural alterations of amide I (1720 to 1580 cm^{-1}), amide II (1580 to 1470 cm^{-1}) and —C—H (1470 to 1350 cm^{-1}) groups, which occurred in the dermis after the topical application of the *F. oxysporum* CE. These spectral modifications may imply that the dermis underwent physicochemical changes that were not observed in the untreated normal skin or the skin on which the culture medium was applied. The region around 1900 to 1700 cm^{-1} was more intense for the 3 and 24 h control samples. One possible explanation for this difference may be the presence of higher amounts of adipose tissues in the illuminated areas. We should stress that this spectral region was not considered in our interpretation. Moreover, Fig. 3 shows the FTIR data in the spectral region between 3850 and 3000 cm^{-1} . It is observed that the OH^- and amine (N—H) bands presented an increase in their intensities with time after the application of both CE and CZ medium. Once these bands are present in both, this result confirms that the CE and CZ medium permeate through the skin reaching the dermal region. Therefore, our hypothesis is that the physicochemical changes in the skin dermal side observed from the FTIR-PAS data strongly suggest that either partial or complete extract permeation occurred and then produced the observed skin structural alterations.

Figure 4 shows the behavior of the peak area at approximately 1370 cm^{-1} within the —CH_3 group region (1350 to

1480 cm^{-1}) for 3, 6, 12, and 24 h after the topical application of the *F. oxysporum* CE. The control point ($t = 0$) represents the peak area of the dermis without the application of any substance. In the infrared region, the —CH_3 group also gives rise to absorption in the 1460 cm^{-1} region. At this frequency, the molecule has an asymmetric bending vibration mode. This group also has vibrational characteristics at 1374 cm^{-1} , which is a symmetric bending vibration mode.³⁶ The spectra obtained for the epidermis and dermis after the application of the CZ medium showed different behavior from that observed after the application of the CE, suggesting that the medium and extract have different contributions to the potential structural changes of the highlighted groups (amide I, amide II, and —CH_3) as evidenced in Fig. 2(b).

Histopathological evaluation did not show macroscopic changes on the skin surfaces of the rats treated with the *F. oxysporum* extract. However, during the microscopic examination of the sections stained with H&E, the following changes were detected: (1) red cells were observed on the surface of the skin (at 3 and 6 h), (2) keratinocytes were present on the epidermis with a bright, perinuclear halo that is typical of hydropic alterations, mainly at 3 h, and (3) the cell number increased on the dermis, and the cells were diffusely localized, particularly for the higher frequencies of fibroblasts and macrophages, but few neutrophils and no formation of typical inflammatory infiltrates were observed, as shown in Fig. 5. The inflammation score is shown in Table 1.

Skin morphometry analysis showed the epidermis of the animals treated with the CE were thicker ($P < 0.05$) after 6, 12, and 24 h [Fig. 6(a)]. The dermis was thicker after 12 and 24 h [Fig. 6(b)]. For the animals treated with the CE and death after 3 and 6 h, the thicknesses of the dermis were significantly reduced [Fig. 6(b)]. Bhavanishankar et al.³⁹ suggested that

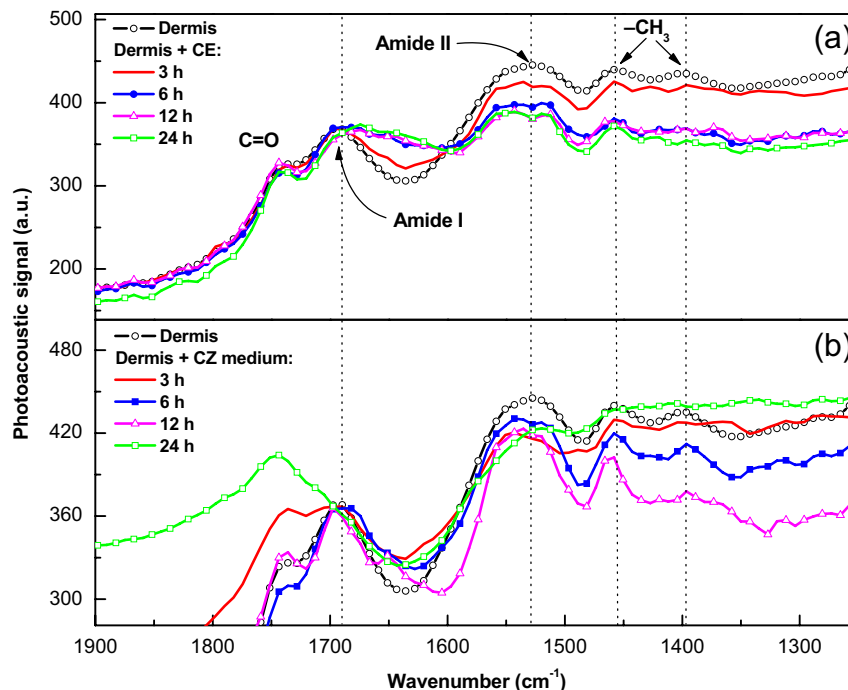


Fig. 2 Spectra of the dermis of rats obtained by Fourier transform infrared photoacoustic spectroscopy (FTIR-PAS) showing the regions corresponding to the amide I (1720 to 1580 cm^{-1}), amide II (1580 to 1470 cm^{-1}), and —CH_3 group (1470 to 1350 cm^{-1}), performed at 3, 6, 12, and 24 h after the topical application of the *F. oxysporum* CE (a) and after the topical application of the CZ culture medium (b). The dermis without any substance applications is also shown.

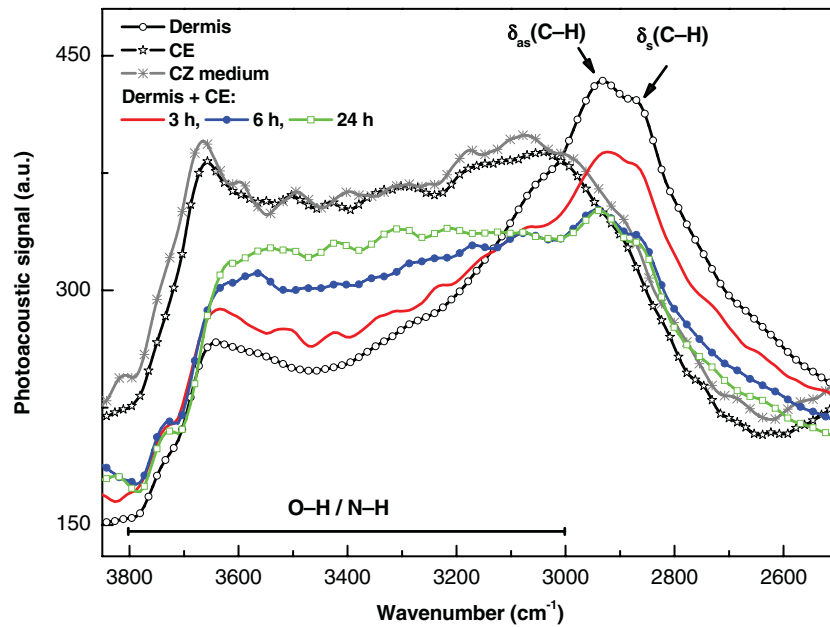


Fig. 3 FTIR-PAS spectra at the range between 2500 and 3750 cm^{-1} of the dermis control, dermis after the topical application of CZ culture medium and dermis at 3, 6, and 24 h after the topical application of the *F. oxysporum* CE.

several toxins produced by *Fusarium* act in different manners when they appear in different combinations. The authors evaluated the variations in epidermis thickness *in vivo* in guinea pigs after the topical application of isolated toxins or a combination of toxins produced by *F. oxysporum*. The epidermal thickening by T2 toxin combined with either FX or butenolide (Bd) was greater than by T2 alone. This finding indicates an antagonistic relationship between these toxins. A greater thickness occurred upon the application of a combination of DAS, which is a trichothecene toxin, and Bd, which is a nontrichothecene toxin, suggesting a synergistic toxic effect by this combination.

In the dermis of the animals treated with the CE, the area covered by collagen type I increased after 3, 6, and 12 h,

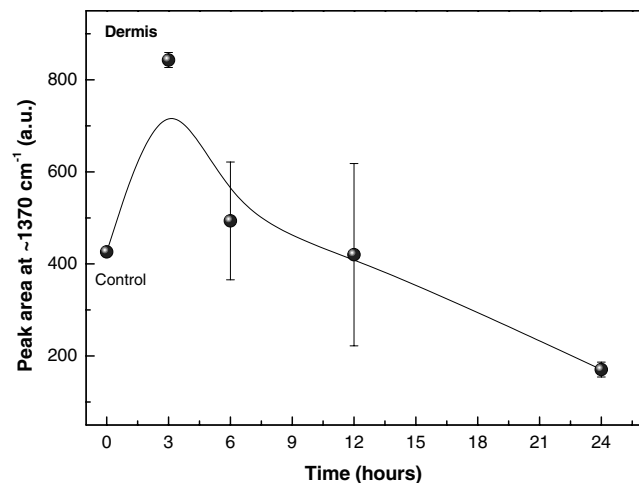


Fig. 4 Behavior of the peak area at approximately 1370 cm^{-1} within the $-\text{CH}_3$ group region (1480 to 1350 cm^{-1}) as a function of time after the application of the CE. The control point ($t = 0$) represents the dermis without the application of the CE. The line is a visual guide.

and the area covered by collagen type III increased after 3, 6, 12, and 24 h compared to the dermis of the animals treated with the culture medium [Fig. 7(a)]. For all the evaluated time points, the total area covered by collagen was larger ($P < 0.05$) in the groups treated with the CE [Fig. 7(b)]. Figure 7(c) shows the proportion of collagen III:I. The greatest disparity in the ratio of the collagen fibers (6 and 24 h) occurs after the maximum for death (3 h) and proliferation (12 h) of fibroblasts. With the death of cells (fibroblasts), the matrix is reabsorbed. A slight decrease in the mature collagen, type I, is observed in skin treated with the CE. With the formation of new cells, a matrix is produced, and the increase in the immature collagen, type III, is observed. In the control group, a balance in the proportions of the types I and III fibers could be observed.

TUNEL immunohistochemical reaction to the stained apoptotic cells results are shown in Table 2 and Figs. 8(a) and 8(b). The basal layer of the epidermis showed the highest frequency and positive intensity after labeling with TUNEL, followed by the Prickle-cell layer and the other layers that had more diffuse labeling. In the dermis, fibroblasts and hair follicles cells were the most immunostained cell types. The strong staining of the follicles was most likely due to its involutive process that occurred after epilation.⁴⁰ A large number of stained cells were observed in the skin tissue and *panniculus carnosus* muscle cells. In a previous study, we reported the occurrence of programmed cell death in these same tissue types after the intradermal administration of a *F. oxysporum* CE that was grown under the same conditions.⁴¹ These results demonstrated the potential permeation capacity through the skin and the harmful effects of this extract, even after a single application.

The capacity of apoptosis induction on basal cells within the epidermis after a topical application of the *Fusarium* T2 toxin was shown in a model of Wistar rats WBN/ILA-Ht.⁴² Albarenque and Doi⁴³ found a 40% decrease in the viability of keratinocytes in primary culture after 3 h, with evolution up to 12 h after the administration of T2 toxin. These authors used an *in vitro* model. Morphological alterations (e.g., chromatin

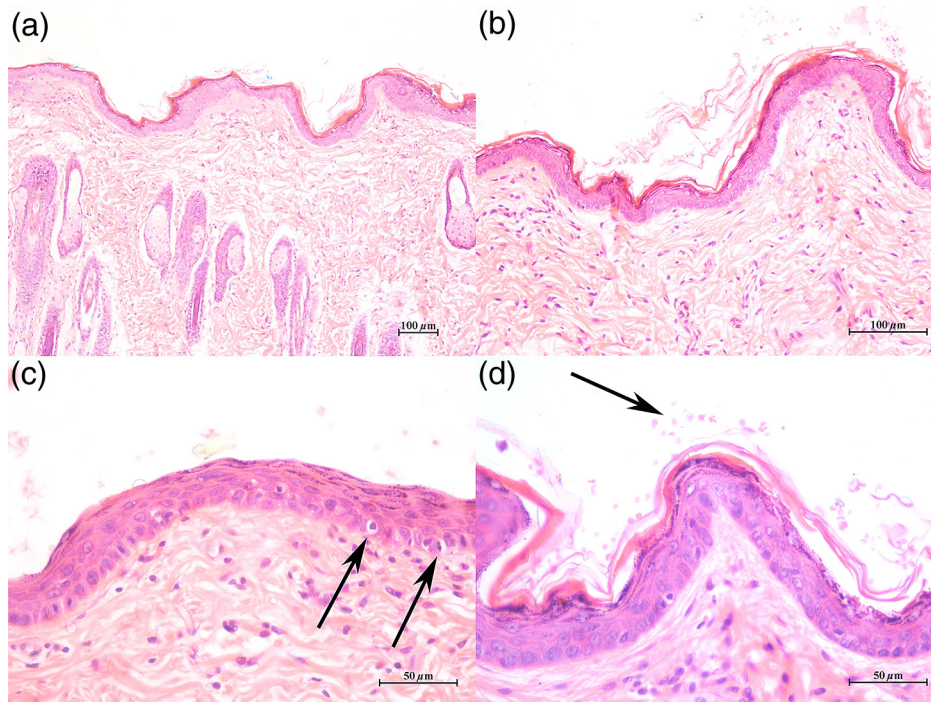


Fig. 5 Rat skin photomicrography after the topical application of the CZ medium (a) or *F. oxysporum* CE (b, c, and d). Note the normal skin morphology 24 h after the medium application in (a). In the skin treated with the CE, the number of dermal cells (b), hydropic alterations (arrows, c), and red cells on the skin surface (arrow, d) increased after 3 h (H&E).

condensation and margination and nuclear fragmentation, all of which are characteristics of cells undergoing apoptosis) were also recorded by optical and electron microscopy. In particular, the potential of programmed cell death induction has been attributed to trichothecenes,^{42–46} which are molecules that have molecular weights of 250 to 500 Da.⁴⁷ In the present study, using a dialysis membrane with a molecular weight cut-off of 12 to 16 kDa may have removed the trichothecenes from the CE; thus, the induction of apoptosis could be attributed to other extracted components with toxic potential. Another hypothesis includes the formation of complexes between smaller molecules that can reach molecular weights >16 kDa. These complexes would not be eliminated in the dialysis process and could maintain their toxic potential, inducing the apoptosis observed by TUNEL.

It is important to observe that the period with higher intensity of TUNEL, 3 h after CE application, coincides with the most pronounced structural changes observed in the FTIR-PAS data, revealed by the modifications in the optical absorption bands associated with the $-\text{CH}_3$ group, at 1370 cm^{-1} . A similar result was detected in the controls, suggesting that there were structural changes that could be related to the process of programmed

cell death in the skin treated with the fungal extract. Marder et al.⁴⁸ reported that the optical absorption band at 1374 cm^{-1} was related to the presence of mycotoxins produced by *B. sorokiniana*.

Table 3 and Figs. 8(c) and 8(d) show the results obtained after the immunohistochemistry reaction to detect anti-PCNA-positive cells. The results showed that there is a thickening of the epidermis within 6, 12, and 24 h after the application of the CE. The strong labeling of PCNA, the expression of which increased in the G1 and S phases of the cell cycle,^{49–52}

Table 1 Score representing the frequency of skin inflammatory cells 3, 6, 12, and 24 h after the topical application of the Czapek–Dox (CZ) medium or the *F. oxysporum* crude extract (CE).

	3 h	6 h	12 h	24 h
CZ	+	++	+++	+
CE	++	+++	++	++

(–) absent, (+) weak, (++) moderate, and (+++) severe.

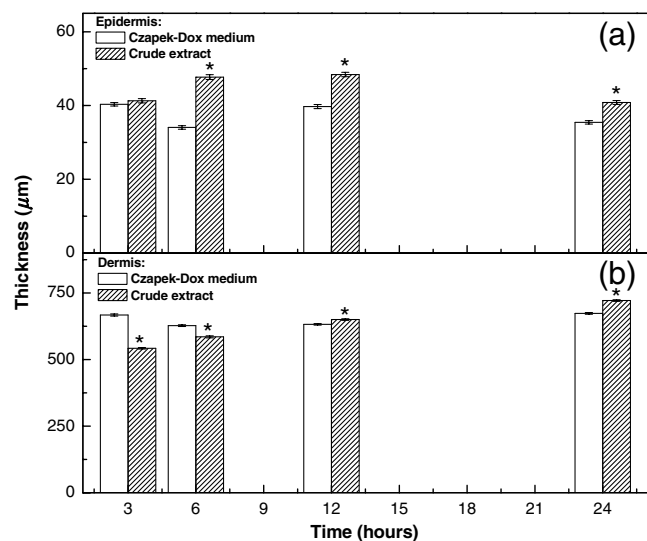


Fig. 6 Thickness measurements (μm) of the epidermis (a) and dermis (b) 3, 6, 12, and 24 h after the topical application of the CZ medium or *F. oxysporum* CE. * $P < 0.05$ when compared to the control at the same time point, $N = 4$ animals/time.

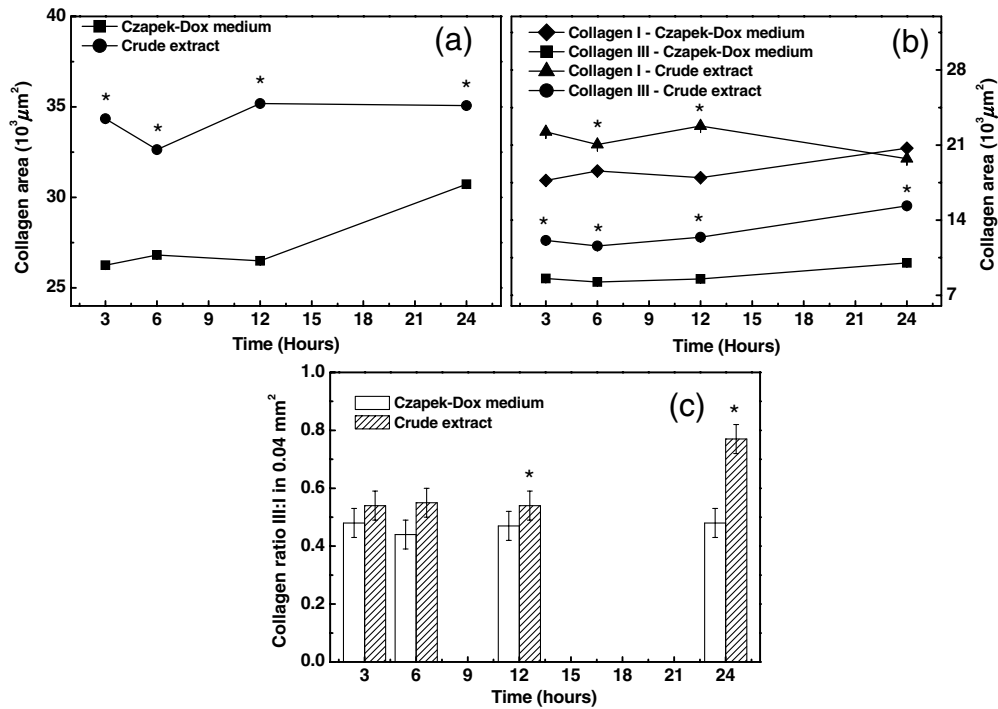


Fig. 7 The area (μm^2) covered by total collagen (a) and types I and III collagen fibers (b) and the proportion of collagen III:I (c) on the dermis of the rats 3, 6, 12, and 24 h after the topical application of the CZ medium or *F. oxysporum* CE. * $P < 0.05$ compared with the control group, $N = 4/\text{time}$.

indicates an increase in the proliferative activity of this tissue after 3 h and moderate labeling after 6, 12, and 24 h. However, as shown above, strong TUNEL was observed at 3 h, and a moderate level of labeling was observed after 6, 12, and 24 h. We believe that the epidermis thickening would reflect the changes in the kinetic activity of the keratinocytes, i.e., stimulating the proliferative activity because of an increased cell death after the topical application of the extract. As shown before, the skin is one of the entrance of *Fusarium*.¹⁶ It is able to break the epithelial barrier inducing cutaneous lesions known as fusariosis.¹⁸ Then, it is reasonable to suppose that the topical application of the CE may be able to temporarily modify the epithelial permeability resulting in cutaneous dehydration because of the higher concentration gradient of the CE in the dermis, with consequent changes in its thickness, as occurred 3 and 6 h after the extract application. In the same period, a number of keratinocytes showed hydropic changes, a reversible state resulting from cellular injury.⁵³

The skin response after topical application differed from that observed after the intradermal inoculation of the *F. oxysporum*

CE. Although the number of inflammatory cells in the dermis increased, there was no formation of typical inflammatory infiltrate. The most frequent inflammatory cells were macrophages, followed by a small number of lymphocytes and neutrophils. These characteristics suggest that the epidermis has exercised its barrier function, preventing the extract from fully permeating.

The dermal fibroblasts were largely responsible for the increased cellularity after the application of the *Fusarium* extract. Fibroblasts are the cells responsible for the production of extracellular matrix components. *In vitro* studies showed that these cells are susceptible to the action of mycotoxins.^{53,54} We observed that the dermal fibroblasts showed strong labeling for cell death after 3 h and moderate labeling in other periods. In contrast, the fibroblasts showed moderate positivity for proliferation at 3 and 6 h, a peak at 12 h, and decay at 24 h. Thus, these results indicate the pursuit of tissue component replacement after the imbalance caused by an external agent. The morphometric analysis of the dermis thickness and the area covered by collagen support this hypothesis because

Table 2 Terminal dUTP nick end labeling immunostaining score of the epidermis and dermis 3, 6, 12, and 24 h after the topical application of the *Fusarium oxysporum* CE or CZ culture medium on the skin of Wistar rats.

	3 h		6 h		12 h		24 h	
	CZ	CE	CZ	CE	CZ	CE	CZ	CE
Epidermis	++	+++	+	++	+	++	+	++
Dermis	+	+++	+	++	+	++	+	++

(-) absent labeling, (+) weak labeling, (++) moderate labeling, and (+++) strong labeling based on the frequency of the stained cells.

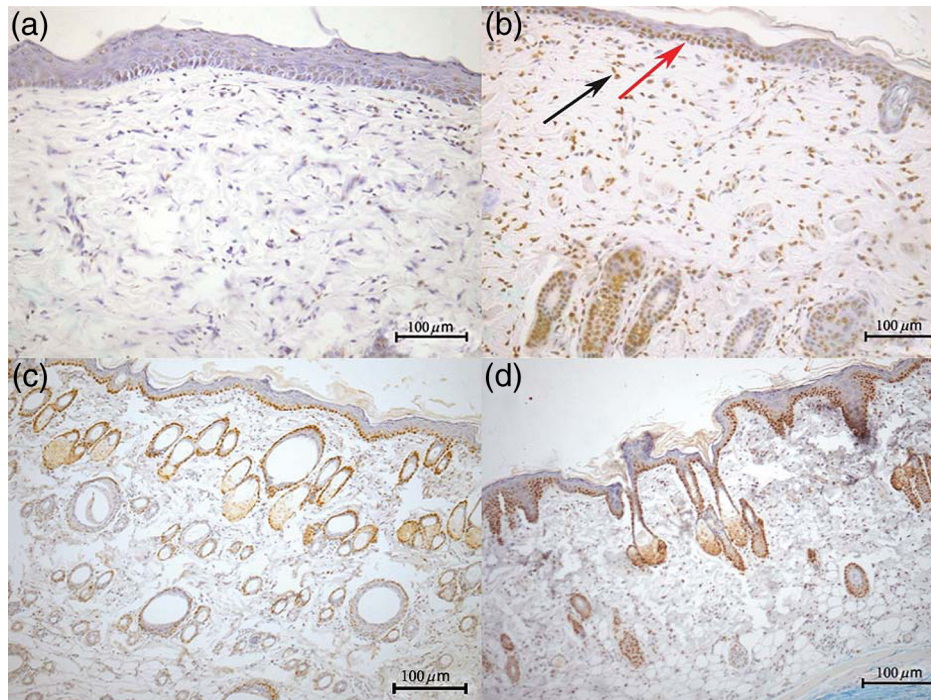


Fig. 8 Rat skin photomicrography 3 h after the topical application of the CZ medium (a, c) or *F. oxysporum* CE (b, d). (b) Terminal dUTP nick end labeling was observed in epidermal keratinocytes (black arrow) and dermal fibroblasts (red arrow). Note the lower frequency of labeling in the control group (a). (c and d) for proliferating cell nuclear antigen immunostaining, note the higher frequency of cells stained (brown stain) on the epidermis of the animals from the group treated with the CE compared to the control group (d).

Table 3 Proliferating cell nuclear antigen immunostaining scores for the epidermis and dermis 3, 6, 12, and 24 h after the topical application of the *F. oxysporum* CE or CZ culture medium on the skin of Wistar rats.

	3 h		6 h		12 h		24 h	
	CZ	CE	CZ	CE	CZ	CE	CZ	CE
Epidermis	+	+++	+	++	++	++	+	++
Dermis	+	++	+	++	++	+++	+	+

(-) absent labeling, (+) weak labeling, (++) moderate labeling, and (+++) strong labeling.

after 12 h, there was significant dermal thickening, which was most likely due to increased collagen synthesis [Fig. 6(b)].

4 Conclusion

In this work, we demonstrated that the *F. oxysporum* CE could permeate the epidermis and dermis, reaching the subcutaneous tissue, inducing apoptosis of the cells in these tissues, and causing physicochemical changes in the organic molecules located in the dermis. Considering that the animals were immunocompetent, the proliferative and morphological changes observed in this study were derived from a process of tissue recovery after the irritating stimulation ended. We believe that the procedure used in this work may be useful for future studies in immunocompromised knockout animals to investigate the dynamics of the physicochemical changes that may occur in the infected tissues.

Acknowledgments

We are thankful to Brazilian agencies CAPES, CNPq, FINEP, and Fundação Araucária for the financial support of this work.

References

1. J. T. Mills, "Ecology of mycotoxigenic *Fusarium* species on cereal seeds," *J. Food Protect.* **52**(10), 737–742 (1989).
2. J. W. Rippon, *Tratado de Micologia Médica*, 3rd ed., Mc Graw Hill, México (1990).
3. J. Guarro and J. Gene, "Opportunistic fusarial infections in humans," *Eur. J. Clin. Microbiol. Infect. Dis.* **14**(9), 741–754 (1995).
4. E. Conková et al., "Fusarial toxins and their role in animal diseases," *Vet. J.* **165**(3), 214–220 (2003).
5. J. Evans et al., "Intracranial fusariosis: a novel cause of fungal meningoencephalitis in a dog," *Vet. Pathol.* **41**(5), 510–514 (2004).
6. S. M. Abdel-Rahman et al., "Pharmacokinetics of terbinafine in young children treated for tinea capitis," *Pediatr. Infect. Dis. J.* **24**(10), 886–891 (2005).
7. M. L. D. F. Perón, J. J. V. Teixeira, and T. I. E. Svidzinski, "Epidemiologia e etiologia das dermatomicoses superficiais e cutâneas na Região de Paranavaí-Paraná, Brasil," *Rev. Bras. Anal. Clin.* **37**(2), 77–81 (2005).
8. J. A. A. Oliveira et al., "Superficial mycoses in the City of Manaus/AM between March and November/2003," *An. Bras. Dermatol.* **81**(3), 238–243 (2006).
9. J. P. F. D'Mello, C. M. Placinta, and A. M. C. MacDonald, "Fusarium micotoxins: a review of global implications for animal health, welfare and productivity," *Anim. Feed Sci. Technol.* **80**(3), 183–205 (1999).

10. C. M. Placinta, J. P. F. D'Mello, and A. M. C. MacDonald, "A review of worldwide contamination of cereal grains and animal feed with *Fusarium* mycotoxins," *Anim. Feed Sci. Technol.* **78**(1), 21–37 (1999).
11. E. C. Hopmans and P. A. Murphy, "Fumonisin: mycotoxins produced by *Fusarium moniliforme*," in *Natural Protectants Against Natural Toxicants*, W. R. Bidlack and S. T. Omaye, Eds., pp. 61–78, Technomic Publishing, Lancaster, Pennsylvania (1993).
12. D. R. Lauren and W. A. Smith, "Stability of 328 *Fusarium* mycotoxins nivalenol, deoxynivalenol and zearalenone in ground maize under typical cooking conditions," *Food Addit. Contam.* **18**(11), 1011–1016 (2001).
13. M. Maresca and J. Fantini, "Some food-associated mycotoxins as potential risk factors in human predisposed to chronic intestinal inflammatory diseases," *Toxicol.* **56**(3), 282–294 (2010).
14. E. E. Creppy et al., "Synergistic effects of fumonisin B1 and ochratoxin A: are in vitro cytotoxicity data predictive of in vivo acute toxicity?," *Toxicology* **201**(1–3), 115–123 (2004).
15. J. H. Kouadio et al., "Effects of combinations of *Fusarium* mycotoxins on the inhibition of macromolecular synthesis, malondialdehyde levels, DNA methylation and fragmentation, and viability in Caco-2 cells," *Toxicol.* **49**(3), 306–317 (2007).
16. A. K. Gupta, R. Baran, and R. C. Summerbell, "Fusarium infection of the skin," *Curr. Opin. Infect. Dis.* **13**(2), 121–128 (2000).
17. E. Guilhermetti et al., "*Fusarium* spp as agents of onychomycosis in immunocompetent hosts," *Int. J. Dermatol.* **46**(8), 822–826 (2007).
18. M. Halpern et al., "Cellulitis and nodular skin lesions due to *Fusarium* spp in liver transplant: case report," *Transplant. Proc.* **42**(2), 599–600 (2010).
19. C. Girmenia et al., "Onychomycosis as a possible origin of disseminated *Fusarium solani* infection in a patient with severe aplastic anemia," *Clin. Infect. Dis.* **14**(5), 1167 (1992).
20. M. Nucci and E. Anaissie, "Cutaneous infection by *Fusarium* species in healthy and immunocompromised hosts: implications for diagnosis and management," *Clin. Infect. Dis.* **35**(8), 909–920 (2002).
21. P. Godoy et al., "Onychomycosis caused by *Fusarium solani* and *Fusarium oxysporum* in São Paulo- Brazil," *Mycopathologia* **157**(3), 287–290 (2004).
22. C. Romano et al., "A case of primary localized cutaneous infection due to *Fusarium oxysporum*," *Mycopathologia* **170**(1), 39–46 (2010).
23. E. I. Boutati and E. I. Anaissie, "Fusarium, a significant emerging pathogen in patients with hematologic malignancy: ten years' experience at a cancer center and implications for management," *Blood* **90**(3), 999–1008 (1997).
24. F. C. Odds et al., "Evaluation of possible correlations between antifungal susceptibilities of filamentous fungi in vitro and antifungal treatment outcomes in animal infection models," *Antimicrob. Agents Chemother.* **42**(2), 282–288 (1998).
25. A. Deshmukh et al., "Raman spectroscopy of normal oral buccal mucosa tissues: study on intact and incised biopsies," *J. Biomed. Opt.* **16**(12), 127004 (2011).
26. J. Kim et al., "In-vitro detection of artificial caries on vertical dental cavity walls using infrared photothermal radiometry and modulated luminescence," *J. Biomed. Opt.* **17**(12), 127001 (2012).
27. S. T. Saito et al., "Study of DNA-emodin interaction by FTIR and UV-vis spectroscopy," *J. Photochem. Photobiol. B* **111**(4), 59–63 (2012).
28. N. Tabatabaei et al., "On the sensitivity of thermophotonic lock-in imaging and polarized Raman spectroscopy to early dental caries diagnosis," *J. Biomed. Opt.* **17**(2), 025002 (2012).
29. X. Pery et al., "In vivo skin solvent penetration measurements using opto-thermal radiometry and fingerprint sensor," *Int. J. Thermophys.* **33**(10–11), 1787–1794 (2012).
30. G. B. Jung et al., "Effect of cross-linking with riboflavin and ultraviolet A on the chemical bonds and ultrastructure of human sclera," *J. Biomed. Opt.* **16**(12), 125004 (2011).
31. E. M. Morato et al., "Morphological and structural changes in lung tissue infected by *Paracoccidioides brasiliensis*: FTIR photoacoustic spectroscopy and histological analysis," *Photochem. Photobiol.* **89**(5), 1170–1175 (2013).
32. A. L. M. Ubaldini et al., "Fourier transform infrared photoacoustic spectroscopy study of physical chemistry interaction between human dentin and etch-&-rinse adhesives in a simulated moist bond technique," *J. Biomed. Opt.* **17**(6), 065002 (2012).
33. M. L. Baesso, R. D. Snook, and J. J. Andrew, "Fourier transform infrared photoacoustic spectroscopy to study the penetration of substances through skin," *J. Phys. IV* **4**(C7), 449–451 (1994).
34. R. D. Snook, R. D. Lowe, and M. L. Baesso, "Photothermal spectrometry for membrane and interfacial region studies," *Analyst* **123**(4), 587–593 (1998).
35. G. Socrates, *Biological Molecules—Macromolecules in Infrared and Raman Characteristic Group Frequencies*, pp. 330–340, John Wiley & Son, Chichester, UK (2001).
36. M. Diem, P. R. Griffiths, and J. M. Chalmers, *Vibrational Spectroscopy for Medical Diagnosis*, John Wiley & Son, Chichester, UK (2008).
37. J. R. Mourant et al., "FTIR spectroscopy demonstrates biochemical differences in mammalian cell cultures at different growth stages," *Biophys. J.* **85**(3), 1938–1947 (2003).
38. S. Xiaoliang et al., "Detection of lung cancer tissue by attenuated total reflection-Fourier transform infrared spectroscopy—a pilot study of 60 samples," *J. Surg. Res.* **179**(1), 33–38 (2013).
39. T. N. Bhavanishankar, H. P. Ramesh, and T. Shantha, "Dermal toxicity of *Fusarium* toxins in combination," *Arch. Toxicology* **61**(3), 241–244 (1988).
40. T. Ito, "Hair follicle is a target of stress hormone and autoimmune reactions," *J. Dermatol. Sci.* **60**(2), 67–73 (2010).
41. A. V. Marangon et al., "Metabolic extract of *Fusarium oxysporum* induces histopathologic alterations and apoptosis in the skin of Wistar rats," *Int. J. Dermatol.* **48**(7), 697–703 (2009).
42. S. M. Albarenque et al., "T-2 toxin-induced acute skin lesions in Wistar-derived hypotrichotic WBN/ILA-Ht rats," *Histol. Histopathol.* **14**(2), 337–342 (1999).
43. S. M. Albarenque and K. Doi, "T-2 toxin-induced apoptosis in rat keratinocyte primary cultures," *Exp. Mol. Pathol.* **78**(12), 144–149 (2005).
44. T. Ihara et al., "Apoptotic cellular damage in mice after T-2 toxin-induced acute toxicosis," *Nat. Toxins.* **5**(4), 141–145 (1997).
45. J. Shinozuka et al., "T-2 toxin-induced apoptosis in lymphoid organs of mice," *Exp. Toxicol. Pathol.* **49**(5), 387–392 (1997).
46. S. M. Albarenque et al., "Kinetics of cytokines mRNAs expression in the dorsal skin of WBN/ILA-Ht rats following topical application of T-2 toxin," *Exp. Toxicol. Pathol.* **53**(4), 271–274 (2001).
47. H. Bigalke and A. Rummel, "Medical aspects of toxin weapons," *Toxicology* **214**(3), 210–220 (2005).
48. L. Marder et al., "Quantitative analysis of total mycotoxins in metabolic extracts of four strains of *Bipolaris sorokiniana* (*Helminthosporium sativum*)," *Proc. Biochem.* **41**(1), 177–180 (2006).
49. R. Bravo and H. Macdonald-Bravo, "Changes in nuclear distribution of cyclin (PCNA) but not its synthesis depend on DNA replication," *EMBO J.* **4**(3), 655–661 (1985).
50. P. Kurki et al., "Expression of proliferating cell nuclear (PCNA)/cyclin during cell cycle," *Exp. Cell Res.* **166**(1), 209–219 (1986).
51. T. Haerslev and G. K. Jacobsen, "Microwave processing for immunohistochemical demonstration of proliferating cell nuclear antigen (PCNA) in formalin-fixed and paraffin-embedded tissue," *Acta Pathol. Microbiol. Immunol. Scand.* **102**(1–6), 395–400 (1994).
52. V. Kumar et al., *Robbins & Cotran Pathologic Basis of Disease*, 8th ed., Elsevier, Philadelphia, Pennsylvania (2010).
53. H. K. Abbas, C. J. Mirocha, and W. T. Shier, "Mycotoxins produced from fungi isolated from foodstuffs and soil: comparison of toxicity in fibroblasts and rat feeding tests," *Appl. Environ. Microbiol.* **48**(3), 654–661 (1984).
54. H. K. Abbas, W. T. Shier, and C. J. Mirocha, "Sensitivity of cultured human and mouse fibroblasts to trichothecenes," *J. Assoc. Off. Anal. Chem.* **67**(3), 607–610 (1984).